Communication

The Homoleptic Curcumin-Copper Single Crystal (ML2): A Long Awaited Cherry on the Cake in the Field of Curcumin Metal Complexes

Antonino Arenaza Corona , Marco A. Obregón Mendoza , William Meza Morales , María Teresa Ramírez Apan , Antonio Nieto Camacho , Rubén A. Toscano , Leidys L. Pérez González , Rubén Sánchez Obregón , Raúl G. Enríquez *

Posted Date: 29 June 2023

doi: 10.20944/preprints202306.2148.v1

Keywords: Curcumin-Copper (II); single crystal; cytotoxicity; antioxidant

Communication

The Homoleptic Curcumin-Copper Single Crystal (ML_2): A Long Awaited Cherry on the Cake in the Field of Curcumin Metal Complexes

Antonino Arenaza-Corona, [a§] Marco A. Obregón-Mendoza, [a§] William Meza-Morales, [b] María Teresa Ramírez-Apan, [a] Antonio Nieto-Camacho, [a] Rubén A. Toscano, [a] Leidys L. Pérez-González, [a] Rubén Sánchez-Obregón, [a] Raúl G. Enríquez, [a*]

[a] Instituto de Química, Universidad Nacional Autónoma de México, Circuito Exterior, Ciudad Universitaria, Ciudad de México, C.P. 04510, México

[b] Department of Chemical Engineering, University of Puerto Rico-Mayaguez, Route 108, Mayaguez, Puerto Rico, USA

* Correspondence: enriquezhabib@gmail.com; Tel.: +52-5556224404

§ These authors contributed equally to this work.

Abstract: The first single crystal structure of the homoleptic copper (II) ML_2 complex (M=Cu (II), L=curcumin) was obtained and its structure was elucidated by X-ray diffraction showing a square planar geometry. The supramolecular arrangement is supported by C-H···O interactions and the solvent (MeOH) plays an important role in stabilizing the crystal packing. The cytotoxic activity of the complex against six cancer cell lines substantially surpasses that of curcumin itself, and it is particularly selective against leukemia (K562) and human glioblastoma (U251) cell lines with similar antioxidant activity to BHT. This constitutes the first crystal structure of pristine curcumin complexed with a metal ion.

Keywords: curcumin-copper (II); single crystal, cytotoxicity, antioxidant

1. Introduction

Curcumin (diferuloylmethane, (1*E*,6*E*)-1,7-*bis*(4-hydroxy-3-methoxyphenyl)-1,6-heptadiene-3,5-dione)[1] is the major components of the Asian spice *Curcuma longa* [2]and has been extensively used in the biologic arena due to multiple purported effects such as antioxidant [3–5], anti-inflammatory [6,7], antiviral [8], antibacterial [9,10], antihypertensive, insulin sensitizer[11,12], cytotoxicity against cancer cell lines and regulation of apoptosis [12–19]. However, this molecule has several disadvantages such as low solubility and therefore, poor bioavailability[20], poor stability and fast metabolism [21,22], leading to hampered clinical applications [23].

Curcumin consists of an heptanoid chain with a conjugate beta-keto-enol system two flanked by two aromatic rings (with an orto-methoxy-phenol system). Different research groups consider phenol groups responsible for their low stability [24](due to quinoid conjugation type). Thus, the focus has been the synthesis of derivatives introducing alkyl (methoxycurcumin, ethoxycurcumin, butoxycurcumin) or acetyl (diacetylcurcumin, DAC)[25,26]. Additionally, to improve the solubility and overtake the bioavailability disadvantage, the formation of complexes with divalent (*e.g.*, Zn^{+2}, Cu^{+2}, Mg^{+2}) [27–30] and more scarcely trivalent (*e.g.*, Fe^{+3}, In^{+3}) metal ions [26,31] has been taken as the principal focus for the synthesis of metal complexes.

Historically, the synthesis of metallic complexes of curcumin began with several metal ions including physiologically relevant ones [27,32] (*e.g.*, Zn, Cu, Mg, Mn, Fe, Se, Ni). However, structural characterizations so far are not conclusive from the solid-state point of view (*i.e.*, Single crystal X-Ray diffraction). Therefore, definitive proof of structural evidence of the coordination (ML, ML_2 or ML_3) between pristine curcumin and a metal ion, was missing until now.

Then, a consistent line of reasoning found in the bibliography is that forming a molecular metal complex consisting of pristine curcumin with a metal ion leads to polymeric arrays due to free phenol

Preprints (www.preprints.org) | NOT PEER-REVIEWED | Posted: 29 June 2023 doi:10.20944/preprints202306.2148.v1

groups[33,34]. Wang *et. al.* derivatized the phenol groups using ethoxy or butoxy groups to obtain the stable copper (II) ML_2 crystals [24]. From the biological point of view, Copper (II) is a necessary element to carry out several biological functions and is found widely distributed in connective tissues and blood vessels. A deficiency of this metal can cause different diseases such as anaemia [35], bone fragility [36], and increased susceptibility to infections [37]. In contrast, an excess (intoxication) of copper, is inconvenient and leads to Wilson's disease[38] and other neurological problems including Alzheimer's disease [39].

We have placed our efforts in the obtention of the curcumin-copper(II) complex, due to the important properties reported in the literature such as antioxidant, anti-inflammatory, antibacterial [40], antiviral and antitumoral [41,42]. The chemical study of this complex has been carried out principally using spectroscopic (solution and solid-state) and spectrometric (ionization) techniques [43]. However, an electron density map derived from the X-ray single-crystal structure is now available. Currently, no reports describe the structural elucidation by single-crystal X-ray diffraction (Cambridge Crystallographic Data Center, 2023) between a curcumin molecule and a metal center in the ML_2 form.

In the obtention of the desired ML_2 complex of curcumin described herein (that we have named a "cherry on the cake"), several factors were considered and each one plays its role in turn. Thus, the chelation capability occurs preferentially at the beta-diketone system rather than at the phenolic groups which render a stable six-membered ring system; a 2:1 strict ligand-metal stoichiometry was used to reduce the competitive participation of phenolic groups; the use of a mild acidic media afforded by the copper acetate was used to avoid nucleophilic participation of phenol groups; the use of methanol as solvent was found adequate after several attempts with other solvents.

2. Results

We are reporting the first molecular structure of a single crystal of copper and pristine curcumin coordinated in the ML_2 form. The synthesis of this complex was carried out as depicted in Scheme 1.

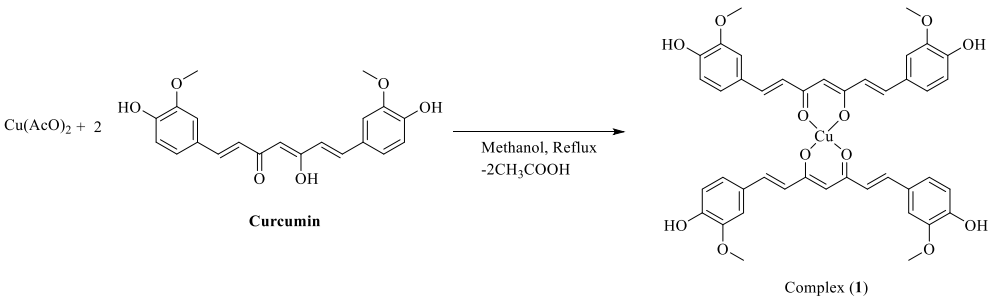

Scheme 1. Formation of ML_2 complex **1** from curcumin.

The solvated (MeOH) structure of curcumin-copper (II) (Complex **1**) crystallized in the triclinic system; space group P-1 (Z = 1) is shown in Figure 1 and the crystallographic data are shown in Table 1. The curcumin (1E,6E)-1,7-bis(4-hydroxy-3-methoxyphenyl)-1,6-heptadiene-3,5-dione), also known with the common name diferuloyl methane exhibits keto–enol tautomerism in solution (MeOH) adopting the enol tautomeric form (1E,4Z,6E)-5-hydroxy-1,7-bis(4-hydroxy-3-methoxyphenyl)hepta-1,4,6-trien-3-one (Scheme 1). Assuming this tautomeric form, Curcumin still has four different rotation axes that can give rise to conformational isomers three of which have been determined by single crystal x-ray diffraction [44,45] (CSC refcodes: BINMEQ, BINMEQ12 and QUMDIN). The anti, s-cis, s-trans, anti-conformation (QUMDIN), where the term anti, indicates the orientations of OCH_3 groups referred to the keto-enol moiety was found for the ligand in its deprotonated form. Although the ligand molecule is nearly planar, the orientations of the phenyl groups are slightly twisted [C6-C7-C14-C15 = -2.1(3)° and C2-C1-C8-C9 = 8.4(4)°].

In the homoleptic complex (**1**), the copper atom resides on an inversion centre with a nearly perfect square planar (τ_4 = 0.00) square planar coordination. The four coordination sites are occupied by oxygen-donor atoms of the 1,6-heptadiene-3,5-dione moieties of curcumins. Thus, each curcumin

Preprints (www.preprints.org) | NOT PEER-REVIEWED | Posted: 29 June 2023 doi:10.20944/preprints202306.2148.v1

acts as a bidentate chelate ligand Figure 1. The corresponding bond lengths are Cu-O1 = 1.9191(15) Å and Cu-O2 = 1.9192(14) Å, O1···O2 = 2.807(2) Å and O1···O2(-x,1-y,1-z) = 2.618(2) Å. The deviation of the mean planes of ligands to the coordination plane is 11.0 °. Selected bond lengths are summarized in Table 2.

Table 1. Crystallographic data of complex **1**.

Empirical formula	**$C_{42}H_{38}O_{12}Cu\cdot5MeOH$**
Formula weight	958.47
Temperature/K	130(2)
Crystal system	*triclinic*
Space group	P-1
a/Å	8.3372(7)
b/Å	8.7677(4)
c/Å	16.3052(12)
α/°	75.664(5)
β/°	84.240(6)
γ/°	84.636(5)
Volume/Å^3	1146.02(14)
Z	1
σ_{calc} g/cm^3	1.389
μ/mm^{-1}	0.551
F(000)	505.0
Crystal size/mm^3	0.33 × 0.13 × 0.06
Radiation	MoKα (λ = 0.71073)
2Θ range for data collection/°	6.852 to 59.284
Index ranges	-11 ≤ h ≤ 11, -12 ≤ k ≤ 11, -22 ≤ l ≤ 22
Reflections collected	25565
Independent reflections	5848 [R_{int} = 0.0466, R_{sigma} = 0.0476]
Data/restraints/parameters	5848/120/377
Goodness-of-fit on F^2	1.047
Final R indexes [I>=2σ (I)]	R_1 = 0.0498, wR_2 = 0.1160
Final R indexes [all data]	R_1 = 0.0706, wR_2 = 0.1293

Table 2. Selected bond lengths [Å] and angles [°] for complex (**1**).

Bond	**length**	**Bond**	**length**
Cu(1)-O(1)	1.9189(15)	C(3)-C(4)	1.407(3)
Cu(1)-O(2)	1.9191(14)	C(4)-C(5)	1.389(3)
O(1)-C(3)	1.280(2)	C(5)-C(6)	1.469(3)
O(2)-C(5)	1.292(2)	C(6)-C(7)	1.344(3)
C(1)-C(2)	1.340(3)	C(7)-C(14)	1.457(3)
C(1)-C(8)	1.458(3)		
C(2)-C(3)	1.466(3)		
Bonds	**Angle**	**Bonds**	**Angle**
O(1)-Cu(1)-O(2)#1	85.99(6)	C(1)-C(2)-C(3)-O(1)	-10.6(3)
O(1)-Cu(1)-O(2)	94.01(6)	C(1)-C(2)-C(3)-C(4)	169.6(2)
C(2)-C(1)-C(8)	126.4(2)	O(1)-C(3)-C(4)-C(5)	7.7(4)
C(1)-C(2)-C(3)	123.3(2)	C(2)-C(3)-C(4)-C(5)	-172.5(2)
O(1)-C(3)-C(4)	124.7(2)	Cu(1)-O(2)-C(5)-C(4)	-5.3(3)
O(1)-C(3)-C(2)	118.2(2)	Cu(1)-O(2)-C(5)-C(6)	175.8(1)
C(4)-C(3)-C(2)	117.1(2)	C(3)-C(4)-C(5)-O(2)	0.0(4)
C(5)-C(4)-C(3)	125.2(2)	C(3)-C(4)-C(5)-C(6)	178.9(2)
O(2)-C(5)-C(4)	124.3(2)	O(2)-C(5)-C(6)-C(7)	-9.4(3)
O(2)-C(5)-C(6)	117.0(2)	C(4)-C(5)-C(6)-C(7)	171.6(2)
C(4)-C(5)-C(6)	118.6(2)	C(5)-C(6)-C(7)-C(14)	175.3(2)
C(7)-C(6)-C(5)	122.2(2)	C(2)-C(1)-C(8)-C(9)	8.5(3)

Preprints (www.preprints.org) | NOT PEER-REVIEWED | Posted: 29 June 2023 doi:10.20944/preprints202306.2148.v1

C(6)-C(7)-C(14)	127.6(2)	C(6)-C(7)-C(14)-C(15)	-2.2(3)

Symmetry transformations are used to generate equivalent atoms: #1 -x,-y+1,-z+1.

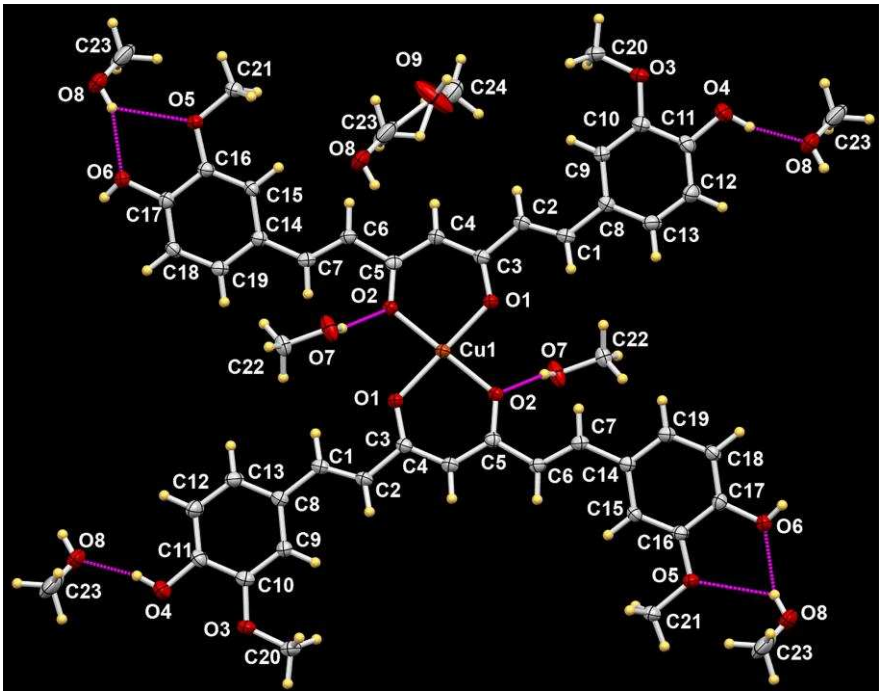

Figure 1. The molecular structure of the complex (**1**) shows the atom labelling, ellipsoids are represented at 50% of probability.

The metal complex (**1**) and pristine curcumin were screened against six cancer cell lines (see supplementary material), and the metal complex was rendered more potent than curcumin itself, with selectivity against leukemia and glial cancer lines. The IC_{50} values were obtained for these two cell lines. The antioxidant tests were recorded in the lipid peroxidation inhibition model (TBARS), showing that the metal complex of curcumin acts against lipid oxidation.

3. Discussion

During the synthesis of the curcumin-copper complex (**1**), our main goal was the obtention of a single crystal of ML_2 type. Both solvent and raw materials were of high purity and a rigorous stoichiometry was used. Additionally, during the process, both the filtrate and the solid precipitate were kept for further workup. Further analysis (see ESI and EPR spectra in supplementary material, Figures S2, S3, S4, S5, S6, S7) showed that both solid and filtrated liquid contained curcuminoid fragments and metal. However, the precipitate was found barely soluble even in large amounts of methanol and rendered an amorphous solid after full evaporation. We attribute this behavior to the possible polymeric nature of the product (m.p. = 280°). On the other hand, the filtrated mother liquor (containing metal-complex and a mixture of acetic acid/methanol) tends to spontaneously form crystals after evaporation and concomitant cooling, and these crystals redissolve readily in methanol at room temperature in an approximately 1:10 w/v ratio. In the latter case, the formation of a single crystal (suitable for X-ray diffraction) was successfully achieved by slow evaporation.

In the crystal structure, the solvent molecules of methanol play key a role in the crystal architecture linking two neighbouring complexes through two strong O4–H4···O8 and O8–H8···O6 hydrogen bonds generating a centrosymmetric cyclic dimer [graph set descriptor: $R_4^4(44)$] which extends infinitely. Furthermore, each 1D infinite chain interacts with two adjacent chains by non-classical hydrogen bonds (C21–H21A···O3 and C21–H21A···O4) forming a 2D sheet parallel to the (2,-1,2) crystallographic plane, Figure 2a. These sheets are interlaced by hydrogen bonds with the second methanol solvent molecule C22–O7 acting as a donor (O7–H7···O2) and acceptor (O6–H6···O7)

Preprints (www.preprints.org) | NOT PEER-REVIEWED | Posted: 29 June 2023 doi:10.20944/preprints202306.2148.v1

generating another centrosymmetric cyclic dimer [graph set descriptor: $R_4^4(28)$] associated to an aromatic ··· metal chelate stacking Figure 2b.

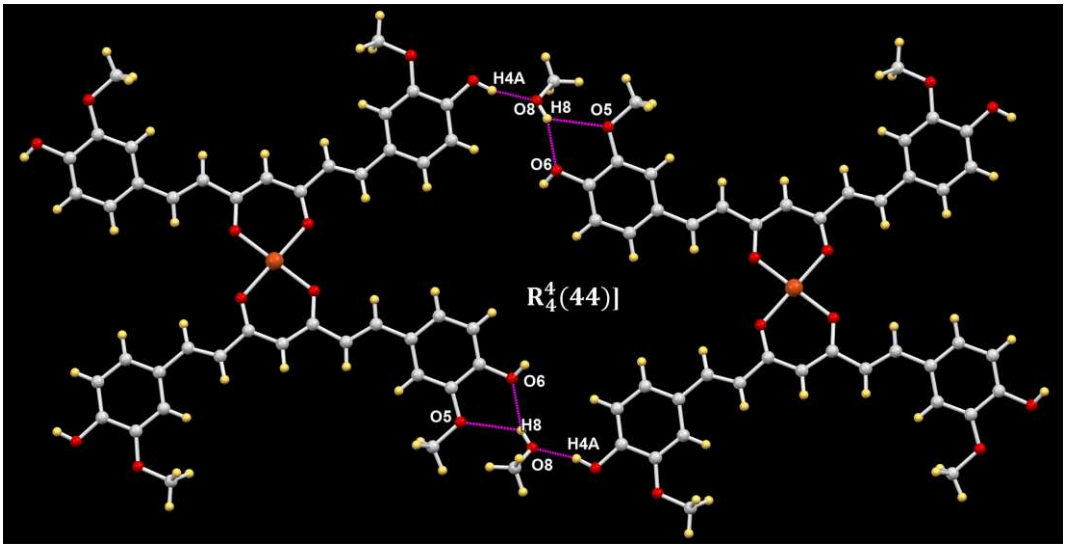

a

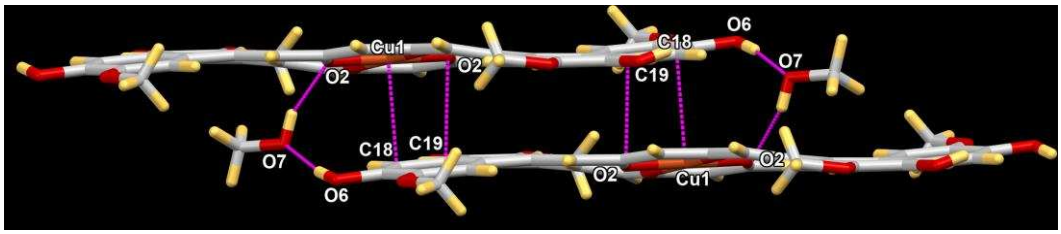

b

Figure 2. A supramolecular arrangement of the complex **1**; top view a, side view b.

The third methanol solvent molecule was found to be disordered around an inversion centre and plays the role of void filling although some contacts can be identified (Table 3).

Table 3. Hydrogen bonds for complex (**1**) [Å and °].

D-H···A	d(D-H)	d(H···A)	d(D···A)	<(DHA)
O(4)-H(4A)...O(8)#1	0.83	1.76	2.552(12)	160.9
O(4)-H(4A)...O(8B)#1	0.83	1.88	2.694(12)	166.7
O(6)-H(6A)...O(7)#2	0.76	2.02	2.767(12)	170.1
O(6)-H(6A)...O(7B)#2	0.76	1.82	2.574(10)	174.9
C(9)-H(9)...O(9B)	0.95	2.52	3.431(9)	161.0
C(18)-H(18)...O(7)#2	0.95	2.53	3.197(12)	127.4
C(20)-H(20A)...O(9B)	0.98	2.41	3.208(9)	138.4
C(21)-H(21A)...O(4)#3	0.98	2.64	3.580(3)	161.1
O(7)-H(7A)...O(2)#4	0.84	1.96	2.734(15)	153.2
O(8)-H(8)...O(5)#5	0.80	2.42	2.988(12)	129.3
O(8)-H(8)...O(6)#5	0.80	2.04	2.801(12)	159.7
C(23)-H(23C)...O(5)#6	0.98	2.46	3.129(10)	125.1

 doi:10.20944/preprints202306.2148.v1

O(7B)-H(7B)...O(2)#4	0.84	1.99	2.786(14)	158.5
O(8B)-H(8B)...O(5)#5	0.84	2.39	3.070(11)	138.5
O(8B)-H(8B)...O(6)#5	0.84	2.11	2.861(11)	148.8
O(9)-H(9A)...O(4)#6	0.83	1.94	2.768(9)	179.3
C(24B)-H(24F)...O(4)#7	0.98	2.62	3.303(13)	126.9

Symmetry transformations used to generate equivalent atoms: #1 x+1,y+1,z; #2 x-1,y-1,z; #3 -x+1,-y+1,-z ; #4 x+1,y,z; #5 x,y+1,z; #6 -x+1,-y+2,-z; #7 x,y-1,z.

To get further information about close contacts in the crystal packing, the Hirshfeld surfaces were mapped using Crystal Explorer software.[46,47]. The surface areas mapped with the shape-index (Figure 3) and the electrostatic potential (Figure 4) functions for the complex revealed close contacts between the phenolic ring and the metal chelate. The blue bump-shape belong to the donor, and the red hollowed spots correspond to the acceptor in an intermolecular interaction.

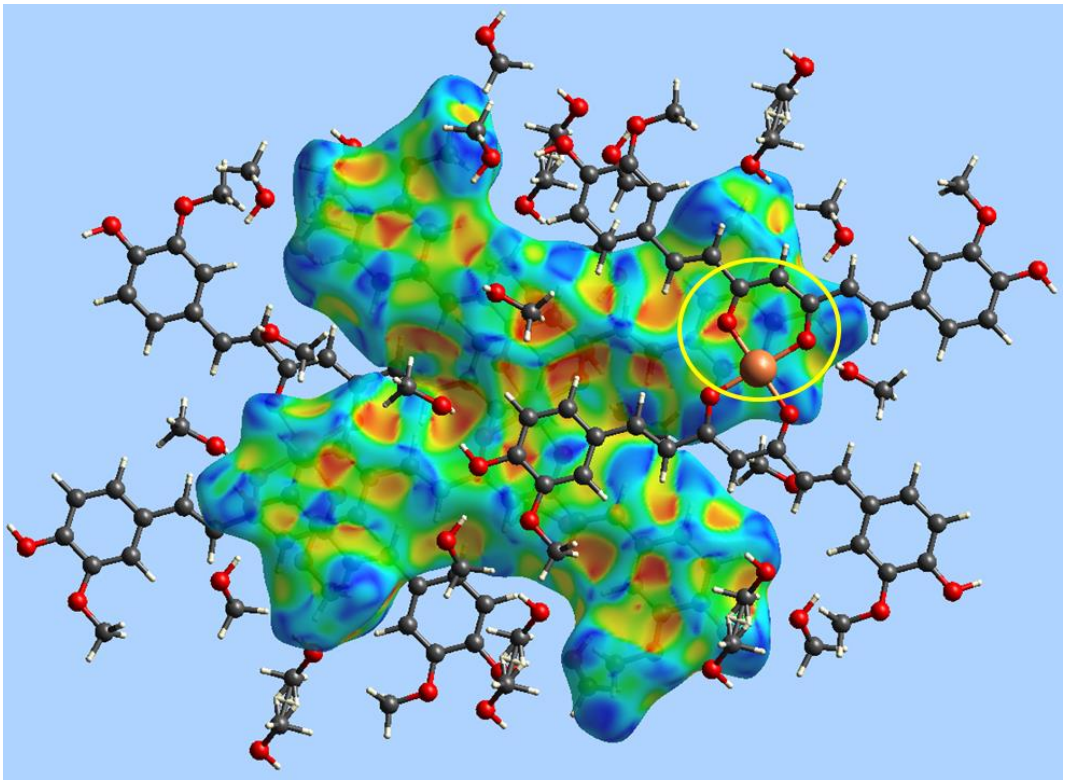

Figure 3. A view of the Hirshfeld surface mapped with the shape-index property illustrating the aromatic...metal chelate interaction (yellow circle).

Preprints (www.preprints.org) | NOT PEER-REVIEWED | Posted: 29 June 2023 doi:10.20944/preprints202306.2148.v1

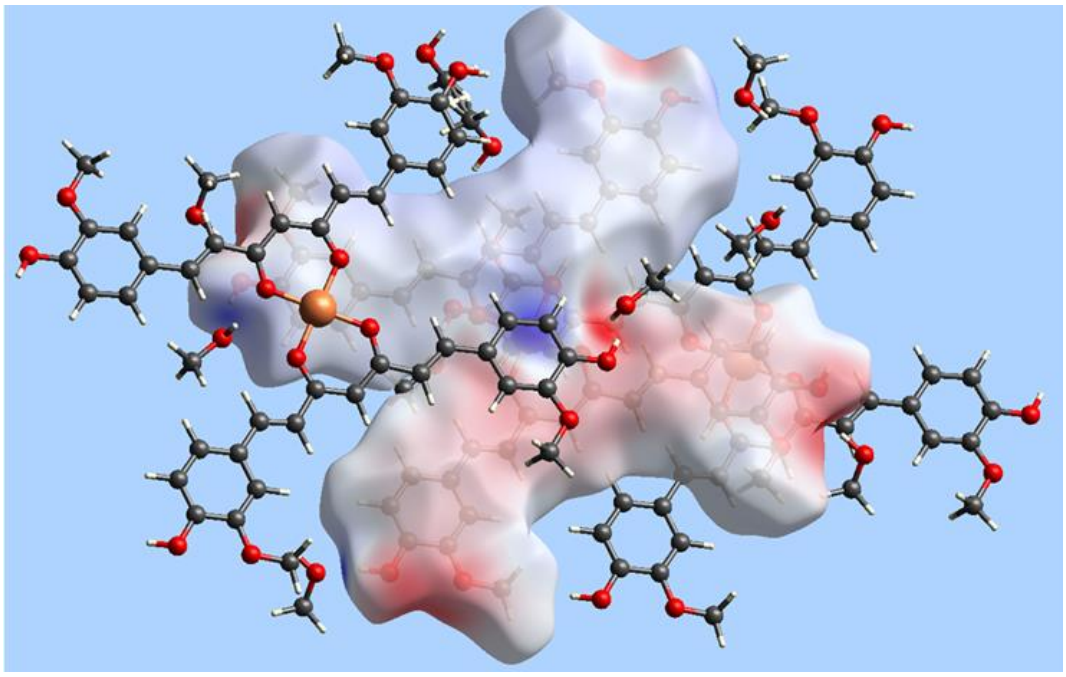

Figure 4. A view of the Hirshfeld surface for (I) mapped over the calculated electrostatic potential in the range -0.1178 to +0.2313 atomic units (the red and blue regions represent negative and positive electrostatic potentials, respectively).

The surface area was determined by the d_{norm} function for the complex, revealing close contacts (red regions) on the phenolic and methoxy groups (Figure 5). However, the 2D fingerprint plot shows the characteristic two peaks corresponding to O···H/H···O contacts (Figure 6a). Also, the greater percentage of contacts originate from H/H interactions followed by O···H/H···O contacts with 44.2 and 24.5 percent respectively (Figure 6b).

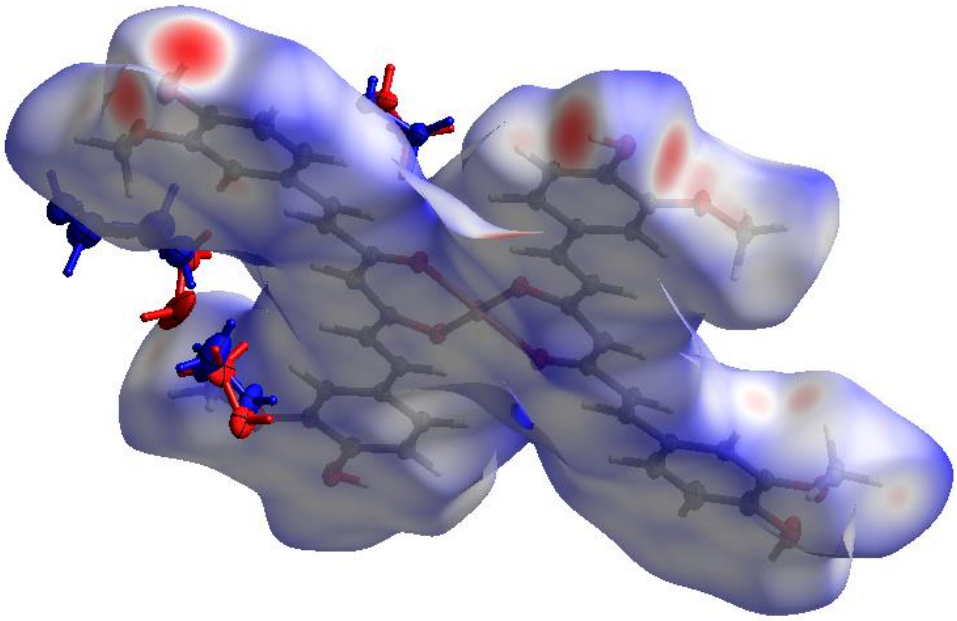

Figure 5. a) Hirshfeld surface (d_{norm}) of complex **1**. Molecules of disordered methanol are represented in red and blue ellipsoids.

Preprints (www.preprints.org) | NOT PEER-REVIEWED | Posted: 29 June 2023 doi:10.20944/preprints202306.2148.v1

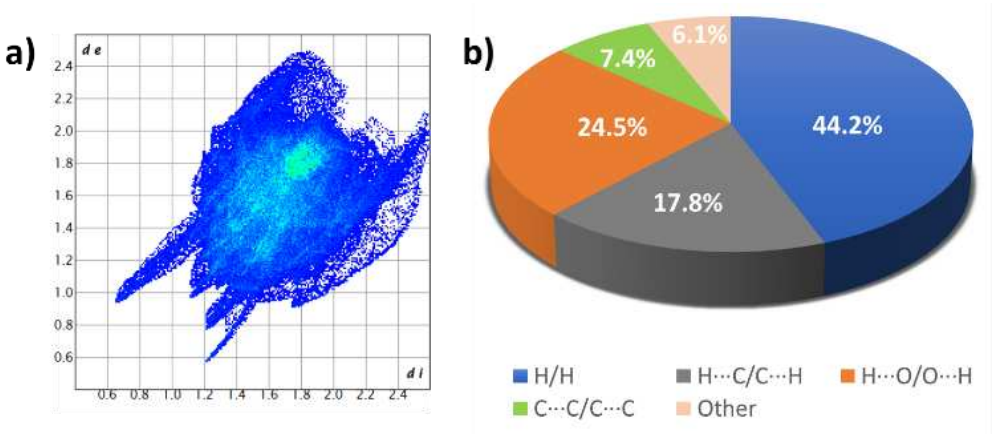

Figure 6. a) a Fingerprint plot of complex **1** from HS and b) an individual percentage of contacts.

A survey for curcumin transition metal complexes on the Cambridge Structural Database, CSD version 5.42 updates (Sep 2021) [48]. shows 23 structures where all of them contain just one molecule of curcumin as a ligand. Of these 23 structures, 8 [49–56](CSD refcodes: PIRVET, HUKGEC, GEGLAH, FEGCOL, BUBSOJ (two molecules), DEYLUR, DOQWUE, GESYAG) display the *anti, s-cis, s-trans, anti* conformation for the ligand. A comparison among this subset including the curcumin ligand (QUMDIN*)* and Compound 1 was performed using the program CrystalCMP [57]. On the calculation of the differences in interatomic distances and the similarity is calculated as a positional difference between molecules in a representative molecular cluster. A very good agreement was found between the structure of ligand in Complex **1** and the corresponding structures found in the subset. A lesser agreement was observed for the pure ligand structure and that found in the complexes (Figure 7).

	0	1	2	3	4	5	6	7	8	9	10	label
0	0.000	1.164	1.103	1.179	1.377	1.436	1.131	1.537	1.554	1.555	0.513	0: 0QUMDIN.CURCUMIN.cif
1	1.164	0.000	0.049	0.088	0.089	0.105	0.111	0.091	0.402	0.418	0.639	1: 1Compound_1.cif
2	1.103	0.049	0.000	0.071	0.221	0.037	0.080	0.167	0.413	0.356	0.511	2: 2PIRVET.AntiAnti.cif
3	1.179	0.088	0.071	0.000	0.150	0.092	0.031	0.145	0.407	0.606	0.617	3: 3HUKGEC.AntiAnti.cif
4	1.377	0.089	0.221	0.150	0.000	0.240	0.169	0.127	0.224	0.202	0.671	4: 4GEGLAH.AntiAnti.cif
5	1.436	0.105	0.037	0.092	0.240	0.000	0.095	0.136	0.291	0.241	0.628	5: 5FEGCOL.AntiAnti.cif
6	1.131	0.111	0.080	0.031	0.169	0.095	0.000	0.280	0.790	0.686	0.589	6: 6BUBSOJ.AntiAnti.cif
7	1.537	0.091	0.167	0.145	0.127	0.136	0.280	0.000	0.408	0.415	0.753	7: 6BUBSOJ.AntiAnti.cif
8	1.554	0.402	0.413	0.407	0.224	0.291	0.790	0.408	0.000	0.047	0.624	8: 6DEYLUR.AntiAnti.cif
9	1.555	0.418	0.356	0.606	0.202	0.241	0.686	0.415	0.047	0.000	0.631	9: 7DOQWUE.AntiAnti.cif
10	0.513	0.639	0.511	0.617	0.671	0.628	0.589	0.753	0.624	0.631	0.000	10: 8GESYAG.AntiAnti.cif

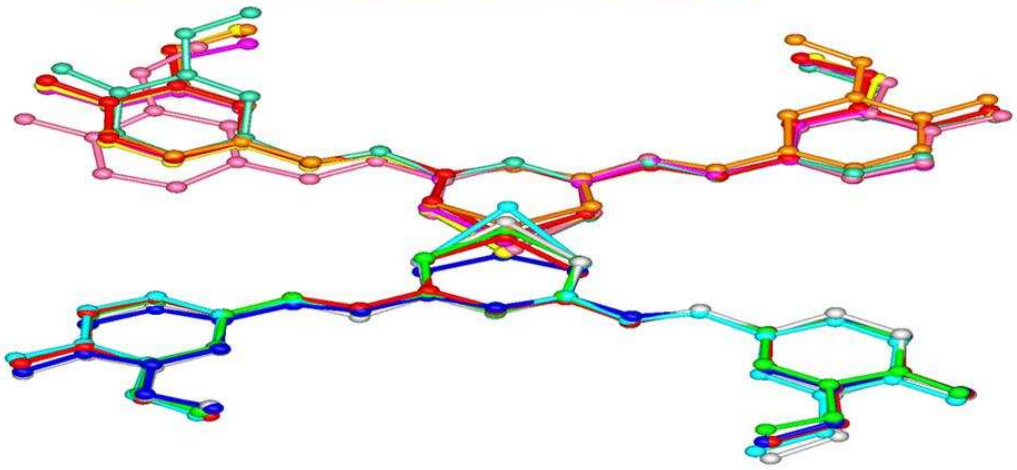

Figure 7. Similarity matrix (top) displaying the RMSD among the crystal structures compared and graphical overlay of these structures (bottom).

 doi:10.20944/preprints202306.2148.v1

Complex **1** was four times more active against the U-251 cell line, see Table 4) than the ligand (curcumin), which agrees with previous reports[58] and suggests that: a) curcumin and the metal ion are mutually stabilized in the complex [27,59,60] and b) solubility and bioavailability are improved [61] and c), the subsequent cell death occurs as a consequence of intercalation with DNA [62].

Table 4. Cytotoxic activity of complex **1** and curcumin.

Complex	**U-251** (IC_{50} = mM)	**K562** (IC_{50} = mM)
Complex (1)	5.3±0.2	9.6±0.3
Curcumin*	20.5±1.7	16.4±0.04

* Taken of reference [63].

The antioxidant assay (TBARS) the copper-complex (**1**) showed enhanced activity with respect to the ligand (almost 3 times, see Table 5) and practically equaled that of BHT (Butylated hydroxytoluene), demonstrating that the copper within the complex plays an important role in the inhibition levels of malondialdehyde (MDA). Also, it is known that the curcumin–Cu^{+2} complex enhances the activities of several antioxidant enzymes (catalase, superoxide dismutase, and glutathione peroxidase) and attenuates the rise of MDA levels [64,65].

Table 5. Antioxidant activity of complex **1** and curcumin.

Complex	IC_{50} = μM)
Complex (1)	1.26±0.08
Curcumin	3.03±0.15
BHT	1.22±0.44

There is a concrete benefit in knowing the precise molecular structure from the X-rays determination of the single crystal of curcumin with copper since it will help to solve structural unknowns (geometry or metal-ligand relationship), as well as to explain different biological effects found, i.e., the antioxidant capacity of the complex, the high cytotoxic potential against cancer cells, and the potential of copper curcumin complex to combat Alzheimer's disease. Furthermore, it will support studies and scope in computational chemistry (QSAR, DFT, molecular docking, etc.).

4. Materials and Methods

Anhydrous copper (II) acetate was available commercially and purchased from Sigma-Aldrich. Pure curcumin was obtained from synthesis as previously reported [66]. The solvents were HPLC grade from Sigma-Aldrich.

4.1. Physical Measurements

The melting points were determined on an Electrothermal Engineering IA9100 × 1 melting point apparatus and are uncorrected.

4.2. Spectroscopic Determinations

The IR-ATR absorption spectra were recorded in the 4000–400 cm^{-1} range on a FT-IR NICOLET IS-50, Thermo Fisher Scientific spectrophotometer. The EPR spectra were recorded in DMSO at liquid nitrogen temperature (77 K) on an Electron Paramagnetic Resonance Spectrometer JEOL, JES-TE300, ITC Cryogenic System, Oxford. Mass spectra were recorded in a Bruker Esquire 6000 with electrospray, atmospheric pressure chemical ionization and ion trap (ESI-TI). Uv-Vis was recorded on UV-VIS SHIMADZU 1800.

4.3. Biological assays

The cytotoxicity of curcumin and curcumin-copper complex **1** was tested against six cancer cell lines: U251 (human glioblastoma cell line), PC-3 (human Caucasian prostate adenocarcinoma), K562

Preprints (www.preprints.org) | NOT PEER-REVIEWED | Posted: 29 June 2023 doi:10.20944/preprints202306.2148.v1

(human Caucasian chronic myelogenous leukaemia), HCT-15 (human colon adenocarcinoma), MCF-7 (human mammary adenocarcinoma), and SKLU-1 (human lung adenocarcinoma). The cell viability in the experiments exceeded 95%, as determined with trypan blue. The human tumour cytotoxicity was determined using the protein-binding dye sulforhodamine B (SRB) in a microculture assay to measure cell growth, as described in the protocols established by the NCI and previously [63]. A dose–response curve was plotted for each complex and the concentration (IC_{50}), resulting in an inhibition of 50% estimated through non-linear regression analysis. Results were expressed as inhibitory concentration 50 (IC_{50}) values.

Antioxidant activity of curcumin and curcumin-copper complex were tested by Thiobarbituric Acid Reactive Substances (TBARS) method and were measured using rat brain homogenates according to the method described by Ng and co-workers [67], with some modifications as previously was recorded [68]. The concentration of TBARS was calculated by interpolation on a standard curve of tetra-methoxypropane (TMP) as a precursor of MDA [69]. Results are expressed as n moles of TBARS per mg of protein. The inhibition ratio (IR [%]) was calculated using the formula IR = (C–E) × 100/C, where C is the control absorbance, and E is the sample absorbance. Butylated hydroxytoluene (BHT) was used as a positive standard. All data are presented as mean ± standard error (SEM). Data were analysed by one-way analysis of variance (ANOVA) followed by Dunnett's test for comparison against control. Values of $p \leq 0.05$ (*) and $p \leq 0.01$ (**) were considered statistically significant.

4.4. Synthesis of complex 1

In a 100 ml ball flask with 30 mL of methanol-HPLC, 200 mg of curcumin was added and heated, and then, a methanolic (50 mL) solution containing 50 mg of anhydrous copper (II) acetate was added dropwise. The mixture was refluxed for 12 h. Then it was concentrated to a volume of approximately 20 mL and this suspension was filtered off in a Hirsch funnel the filtrate, solid was washed with cold methanol-water (8:2 v/v) and was left to stand at *vacuum* and room temperature for four hours. Solid phase: Amorphous solid, dark brown colour, Yield= 20%. Melting point: 285 Celsius. MS (ESI^+) = 797.0 m/z $[M]^+$, 900.9 m/z. IR-ATR 3441 (O-H, phenol), 1491 (C=O-Cu), 965 (C–O, β-diketone) cm^{-1}, 469 cm^{-1} (O-Cu).

Mother liquor (Liquid phase), a solid crystal was obtained in the bottom of the flask and then was cooled with ice and filtered in a Hirsch funnel, the crystals were washed with cold methanol-water (8:2 v/v). And was left to stand at *vacuum* and room temperature for four hours. Crystals, bright brown colour, Yield= 50%. Melting point: 230 Celsius. MS (ESI^+) = 820.0 m/z $[M+Na]^+$, 898.0 m/z $[[M+Na+DMSO]^+$. IR-ATR 3587 (O-H, phenol), 3443 (O-H, MeOH), 1496 (C=O-Cu) cm^{-1}, 963 (C–O, β -diketone), 478 cm^{-1} (O-Cu). Elemental Analysis: Calculated for $C_{42}H_{38}CuO_{12}$·MeOH: C 62.20; H 5.10; experimental: 62.43; H 4.85.

Single crystals formation (suitable for X-ray diffraction), 30 mg of crystals described previously were dissolved in 30 mL of anhydrous methanol -HPLC and filtered for elimination of solid impurities, this solution was left at room temperature with slow evaporation for one week.

4.5. X-ray Crystallography

The diffraction data were collected for 1 on a Rigaku Xcalibur, Gemini with MoKα radiation (λ = 0.71073 Å) by performing ω scans frames at 130 K. Absorption correction was carried out empirically using SCALE3 ABSPACK scaling algorithm (CrysAlisPro, Agilent Technologies, Version 1.171.36.32[70] and refined by full-matrix least-squares treatment against |F|2 in anisotropic approximation with SHELXL-2019/3 [71] in the ShelXle program [72]. H-atoms were included in the geometrically calculated positions.

Conclusions

We have successfully achieved the synthesis and the complete structure elucidation of the homoleptic ML_2 curcumin-copper complex, authenticated through single crystal X-ray diffraction,

unequivocally demonstrating the 2:1 curcumin-metal ratio. An outstanding feature is that no substitution of the phenolic groups was necessary.

The supramolecular analysis demonstrates that the solvent plays a critical role in crystallization. Furthermore, the mother liquor (filtrate) should be considered a suitable source of crystals and not be underestimated.

The biological activity of the homoleptic curcumin-metal complex shows a dramatic increase in cytotoxicity and antioxidant properties compared to pristine curcumin. Therefore, the search for other homoleptic crystal structures of curcumin with different metals is a task to be undertaken in the short future.

Therapeutic areas such as Alzheimer's disease, degenerative neurological ailments, cancer research, and the search for antioxidant agents may hopefully expand their scope from the present finding.

Supplementary Materials: The following are available online. CCDC 2271944 contain the supplementary crystallographic data for this paper. These data can be obtained free of charge via **www.ccdc.cam.ac.uk/cgi-bin/catreq.cgi**, by e-mailing data_request@ccdc.cam.ac.uk, or by contacting: The Cambridge Crystallographic Data Centre, 12 Union Road, Cambridge CB2 1EZ, UK, Fax; +44(0)-1223-336033.

Author Contributions: Antonino Arenaza-Corona: Investigation, Formal analysis, Writing – original draft, Writing – review & editing. **Marco A. Obregón-Mendoza:** Investigation, Formal analysis, Writing – original draft, Writing – review & editing. **William Meza-Morales:** Investigation, Formal analysis. **María Teresa Ramírez-Apan:** Investigation, Formal analysis. **Antonio Nieto-Camacho:** Investigation, Formal analysis. **Rubén A. Toscano:** Investigation, Validation, Formal analysis. **Ruben Sánchez-Obregón:** Investigation, Formal analysis, Writing – original draft. **Leidys L. Pérez-González:** Investigation. **Raúl G. Enríquez:** Conceptualization, Methodology, Formal analysis, Validation, Writing – original draft, Writing – review & editing, Visualization, Supervision, Project administration, Funding acquisition.

Funding: This research was funded by CONAHCyT FOINS-307152 and DGAPA PAPIIT-IT200720.

Institutional Review Board Statement: Not applicable.

Informed Consent Statement: Not applicable.

Data Availability Statement: Not applicable.

Acknowledgements: A.A.C. is grateful to CONAHCyT for the postdoctoral fellowship (CVU: 565984). R.G.E. Thanks for the financing of CONAHCyT FOINS-307152 and DGAPA PAPIIT-IT200720. M.A.O.M. thanks for the payment of project fees CONAHCyT FOINS-307152. L.L.P.G is grateful to CONAHCyT (CVU: 1234478). We are indebted to María de la Paz Orta Perez (AE), Adriana Romo (IR), Virginia Gómez Vidales (EPR), and Lucero Rios Ruiz (ESI) from Instituto de Química, UNAM. USAII, Facultad de Química-UNAM for X-Ray data collection. MVZ Claudia V. Rivera Cerecedo and MVZ Héctor Malagón Rivero from Bioterio de Fisiología Celular (UNAM) for providing the rat brain.

Conflicts of Interest: The authors declare no conflict of interest.

Sample Availability: A sample of complex **1** is available from the authors.

References

1. Hewlings, S.J.; Kalman, D.S. Curcumin: A Review of Its Effects on Human Health. *Foods* 2017, *6*.
2. Prasad, S.; Dubourdieu, D.; Srivastava, A.; Kumar, P.; Lall, R. Metal–Curcumin Complexes in Therapeutics: An Approach to Enhance Pharmacological Effects of Curcumin. *Int J Mol Sci* 2021, *22*.
3. Mishra, S.; Palanivelu, K. The Effect of Curcumin (Turmeric) on Alzheimer's Disease: An Overview. *Ann Indian Acad Neurol* **2008**, *11*, 13, doi:10.4103/0972-2327.40220.
4. Boarescu; Boarescu; Bocșan; Gheban; Bulboacă; Nicula; Pop; Râjnoveanu; Bolboacă Antioxidant and Anti-Inflammatory Effects of Curcumin Nanoparticles on Drug-Induced Acute Myocardial Infarction in Diabetic Rats. *Antioxidants* **2019**, *8*, 504, doi:10.3390/antiox8100504.
5. Hussain, H.; Ahmad, S.; Shah, S.W.A.; Ullah, A.; Rahman, S.U.; Ahmad, M.; Almehmadi, M.; Abdulaziz, O.; Allahyani, M.; Alsaiari, A.A.; et al. Synthetic Mono-Carbonyl Curcumin Analogues Attenuate Oxidative Stress in Mouse Models. *Biomedicines* **2022**, *10*, 2597, doi:10.3390/biomedicines10102597.

6. Witika, B.A.; Makoni, P.A.; Matafwali, S.K.; Mweetwa, L.L.; Shandele, G.C.; Walker, R.B. Enhancement of Biological and Pharmacological Properties of an Encapsulated Polyphenol: Curcumin. *Molecules* **2021**, *26*, 4244, doi:10.3390/molecules26144244.
7. Ghosh, S.; Banerjee, S.; Sil, P.C. The Beneficial Role of Curcumin on Inflammation, Diabetes and Neurodegenerative Disease: A Recent Update. *Food and Chemical Toxicology* **2015**, *83*, 111–124, doi:10.1016/j.fct.2015.05.022.
8. Chauhan, G.; Rath, G.; Goyal, A.K. *In-Vitro* Anti-Viral Screening and Cytotoxicity Evaluation of Copper-Curcumin Complex. *Artif Cells Nanomed Biotechnol* **2013**, *41*, 276–281, doi:10.3109/21691401.2012.742096.
9. Reddy, R.C.; Vatsala, P.G.; Keshamouni, V.G.; Padmanaban, G.; Rangarajan, P.N. Curcumin for Malaria Therapy. *Biochem Biophys Res Commun* **2005**, *326*, 472–474, doi:10.1016/j.bbrc.2004.11.051.
10. Mahady GB, P.S.Y.G.L.Z. Turmeric (Curcuma Longa) and Curcumin Inhibit the Growth of Helicobacter Pylori, a Group 1 Carcinogen. *Anticancer Res* **2002**, *22*, 4179–4181.
11. Ghorbani, Z.; Hekmatdoost, A.; Mirmiran, P. Anti-Hyperglycemic and Insulin Sensitizer Effects of Turmeric and Its Principle Constituent Curcumin. *Int J Endocrinol Metab* **2014**, *12*, doi:10.5812/ijem.18081.
12. Quispe, C.; Herrera-Bravo, J.; Javed, Z.; Khan, K.; Raza, S.; Gulsunoglu-Konuskan, Z.; Daştan, S.D.; Sytar, O.; Martorell, M.; Sharifi-Rad, J.; et al. Therapeutic Applications of Curcumin in Diabetes: A Review and Perspective. *Biomed Res Int* 2022, *2022*.
13. Lei, F.; Li, P.; Chen, T.; Wang, Q.; Wang, C.; Liu, Y.; Deng, Y.; Zhang, Z.; Xu, M.; Tian, J.; et al. Recent Advances in Curcumin-Loaded Biomimetic Nanomedicines for Targeted Therapies. *J Drug Deliv Sci Technol* **2023**, *80*, 104200, doi:10.1016/j.jddst.2023.104200.
14. de Waure, C.; Bertola, C.; Baccarini, G.; Chiavarini, M.; Mancuso, C. Exploring the Contribution of Curcumin to Cancer Therapy: A Systematic Review of Randomized Controlled Trials. *Pharmaceutics* 2023, *15*.
15. Kong, W.-Y.; Ngai, S.C.; Goh, B.-H.; Lee, L.-H.; Htar, T.-T.; Chuah, L.-H. Is Curcumin the Answer to Future Chemotherapy Cocktail? *Molecules* **2021**, *26*, 4329, doi:10.3390/molecules26144329.
16. Zoi, V.; Galani, V.; Lianos, G.D.; Voulgaris, S.; Kyritsis, A.P.; Alexiou, G.A. The Role of Curcumin in Cancer Treatment. *Biomedicines* **2021**, *9*, 1086, doi:10.3390/biomedicines9091086.
17. Jalili-Nik, M.; Soltani, A.; Moussavi, S.; Ghayour-Mobarhan, M.; Ferns, G.A.; Hassanian, S.M.; Avan, A. Current Status and Future Prospective of Curcumin as a Potential Therapeutic Agent in the Treatment of Colorectal Cancer. *J Cell Physiol* **2018**, *233*, 6337–6345, doi:10.1002/jcp.26368.
18. Devassy, J.G.; Nwachukwu, I.D.; Jones, P.J.H. Curcumin and Cancer: Barriers to Obtaining a Health Claim. *Nutr Rev* **2015**, *73*, 155–165, doi:10.1093/nutrit/nuu064.
19. Ravindran, J.; Prasad, S.; Aggarwal, B.B. Curcumin and Cancer Cells: How Many Ways Can Curry Kill Tumor Cells Selectively? *AAPS J* **2009**, *11*, 495–510, doi:10.1208/s12248-009-9128-x.
20. Anand, P.; Kunnumakkara, A.B.; Newman, R.A.; Aggarwal, B.B. Bioavailability of Curcumin: Problems and Promises. *Mol Pharm* **2007**, *4*, 807–818, doi:10.1021/mp700113r.
21. Prasad, S.; Tyagi, A.K.; Aggarwal, B.B. Recent Developments in Delivery, Bioavailability, Absorption and Metabolism of Curcumin: The Golden Pigment from Golden Spice. *Cancer Res Treat* **2014**, *46*, 2–18, doi:10.4143/crt.2014.46.1.2.
22. Sohn, S.-I.; Priya, A.; Balasubramaniam, B.; Muthuramalingam, P.; Sivasankar, C.; Selvaraj, A.; Valliammai, A.; Jothi, R.; Pandian, S. Biomedical Applications and Bioavailability of Curcumin—An Updated Overview. *Pharmaceutics* **2021**, *13*, 2102, doi:10.3390/pharmaceutics13122102.
23. Shen, L.; Ji, H.-F. The Pharmacology of Curcumin: Is It the Degradation Products? *Trends Mol Med* **2012**, *18*, 138–144, doi:10.1016/j.molmed.2012.01.004.
24. Wang, J.; Wei, D.; Jiang, B.; Liu, T.; Ni, J.; Zhou, S. Two Copper(II) Complexes of Curcumin Derivatives: Synthesis, Crystal Structure and in Vitro Antitumor Activity. *Transition Metal Chemistry* **2014**, *39*, 553–558, doi:10.1007/s11243-014-9831-z.
25. Basile, V.; Ferrari, E.; Lazzari, S.; Belluti, S.; Pignedoli, F.; Imbriano, C. Curcumin Derivatives: Molecular Basis of Their Anti-Cancer Activity. *Biochem Pharmacol* **2009**, *78*, 1305–1315, doi:10.1016/j.bcp.2009.06.105.
26. Medigue, N.E.H.; Bouakouk-Chitti, Z.; Bechohra, L.L.; Kellou-Taïri, S. Theoretical Study of the Impact of Metal Complexation on the Reactivity Properties of Curcumin and Its Diacetylated Derivative as Antioxidant Agents. *J Mol Model* **2021**, *27*, 192, doi:10.1007/s00894-021-04768-3.
27. Wanninger, S.; Lorenz, V.; Subhan, A.; Edelmann, F.T. Metal Complexes of Curcumin - Synthetic Strategies, Structures and Medicinal Applications. *Chem Soc Rev* **2015**, *44*, 4986–5002, doi:10.1039/c5cs00088b.
28. Barik, A.; Mishra, B.; Kunwar, A.; Kadam, R.M.; Shen, L.; Dutta, S.; Padhye, S.; Satpati, A.K.; Zhang, H.Y.; Indira Priyadarsini, K. Comparative Study of Copper(II)-Curcumin Complexes as Superoxide Dismutase Mimics and Free Radical Scavengers. *Eur J Med Chem* **2007**, *42*, 431–439, doi:10.1016/j.ejmech.2006.11.012.
29. H. M. Leung, M.; Harada, T.; W. Kee, T. Delivery of Curcumin and Medicinal Effects of the Copper(II)-Curcumin Complexes. *Curr Pharm Des* **2013**, *19*, 2070–2083, doi:10.2174/138161213805289237.

30. Vajragupta, O. Manganese Complexes of Curcumin and Its Derivatives: Evaluation for the Radical Scavenging Ability and Neuroprotective Activity. *Free Radic Biol Med* **2003**, *35*, 1632–1644, doi:10.1016/j.freeradbiomed.2003.09.011.
31. Khalil, M.I.; Al-Zahem, A.M.; Al-Qunaibit, M.H. Synthesis, Characterization, Mössbauer Parameters, and Antitumor Activity of Fe(III) Curcumin Complex. *Bioinorg Chem Appl* **2013**, *2013*, 1–5, doi:10.1155/2013/982423.
32. Al-Noor, T.H.; Ali, A.M.; Al-Sarray, A.J.A.; Al-Obaidi, O.H.; Obeidat, A.I.M.; Habash, R.R. A Short Review: Chemistry of Curcumin and Its Metal Complex Derivatives. **2022**.
33. Portolés-Gil, N.; Lanza, A.; Aliaga-Alcalde, N.; Ayllón, J.A.; Gemmi, M.; Mugnaioli, E.; López-Periago, A.M.; Domingo, C. Crystalline Curcumin BioMOF Obtained by Precipitation in Supercritical CO2 and Structural Determination by Electron Diffraction Tomography. *ACS Sustain Chem Eng* **2018**, *6*, 12309–12319, doi:10.1021/acssuschemeng.8b02738.
34. Su, H.; Sun, F.; Jia, J.; He, H.; Wang, A.; Zhu, G. A Highly Porous Medical Metal–Organic Framework Constructed from Bioactive Curcumin. *Chemical Communications* **2015**, *51*, 5774–5777, doi:10.1039/C4CC10159F.
35. Wazir, S.M.; Ghobrial, I. Copper Deficiency, a New Triad: Anemia, Leucopenia, and Myeloneuropathy. *J Community Hosp Intern Med Perspect* **2017**, *7*, 265–268, doi:10.1080/20009666.2017.1351289.
36. Sierpinska, T.; Konstantynowicz, J.; Orywal, K.; Golebiewska, M.; Szmitkowski, M. Copper Deficit as a Potential Pathogenic Factor of Reduced Bone Mineral Density and Severe Tooth Wear. *Osteoporosis International* **2014**, *25*, 447–454, doi:10.1007/s00198-013-2410-x.
37. Percival, S. Copper and Immunity. *Am J Clin Nutr* **1998**, *67*, 1064S-1068S, doi:10.1093/ajcn/67.5.1064S.
38. Collins, J.F.; Klevay, L.M. Copper. *Advances in Nutrition* **2011**, *2*, 520–522, doi:10.3945/an.111.001222.
39. Desai, V.; Kaler, S.G. Role of Copper in Human Neurological Disorders. *Am J Clin Nutr* **2008**, *88*, 855S-858S, doi:10.1093/ajcn/88.3.855S.
40. Xu, G.; Wang, J.; Liu, T.; Wang, M.; Zhou, S.; Wu, B.; Jiang, M. Synthesis and Crystal Structure of a Novel Copper(II) Complex of Curcumin-Type and Its Application in in Vitro and in Vivo Imaging. *J Mater Chem B* **2014**, *2*, 3659–3666, doi:10.1039/c4tb00133h.
41. Pi, Z.; Wang, J.; Jiang, B.; Cheng, G.; Zhou, S. A Curcumin-Based TPA Four-Branched Copper(II) Complex Probe for in Vivo Early Tumor Detection. *Materials Science and Engineering C* **2015**, *46*, 565–571, doi:10.1016/j.msec.2014.10.061.
42. Zhang, W.; Chen, C.; Shi, H.; Yang, M.; Liu, Y.; Ji, P.; Chen, H.; Tan, R.X.; Li, E. Curcumin Is a Biologically Active Copper Chelator with Antitumor Activity. *Phytomedicine* **2016**, *23*, 1–8, doi:10.1016/j.phymed.2015.11.005.
43. Angulo, J.; Delgado-Villanueva, J. Preparación y Caracterización de Complejos de Curcumina Con Zinc(II), Níquel(II), Magnesio(II), Cobre(II) y Su Evaluación Frente a Bacterias Grampositiva y Gramnegativa. *Revista Politécnica* **2023**, *51*, 63–72, doi:10.33333/rp.vol51n2.06.
44. Su, H.; He, H.; Tian, Y.; Zhao, N.; Sun, F.; Zhang, X.; Jiang, Q.; Zhu, G. Syntheses and Characterizations of Two Curcumin-Based Cocrystals. *Inorg Chem Commun* **2015**, *55*, 92–95, doi:10.1016/j.inoche.2015.03.027.
45. Matlinska, M.A.; Wasylishen, R.E.; Bernard, G.M.; Terskikh, V. V.; Brinkmann, A.; Michaelis, V.K. Capturing Elusive Polymorphs of Curcumin: A Structural Characterization and Computational Study. *Cryst Growth Des* **2018**, *18*, 5556–5563, doi:10.1021/acs.cgd.8b00859.
46. McKinnon, J.J.; Jayatilaka, D.; Spackman, M.A. Towards Quantitative Analysis of Intermolecular Interactions with Hirshfeld Surfaces. *Chemical Communications* **2007**, 3814–3816, doi:10.1039/b704980c.
47. Spackman, M.A.; McKinnon, J.J. Fingerprinting Intermolecular Interactions in Molecular Crystals. *CrystEngComm* **2002**, *4*, 378–392, doi:10.1039/b203191b.
48. Allen, F.H. The Cambridge Structural Database: A Quarter of a Million Crystal Structures and Rising. *Acta Crystallogr B* **2002**, *58*, 380–388, doi:10.1107/S0108768102003890.
49. Caruso, F.; Rossi, M.; Benson, A.; Opazo, C.; Freedman, D.; Monti, E.; Gariboldi, M.B.; Shaulky, J.; Marchetti, F.; Pettinari, R.; et al. Ruthenium-Arene Complexes of Curcumin: X-Ray and Density Functional Theory Structure, Synthesis, and Spectroscopic Characterization, in Vitro Antitumor Activity, and DNA Docking Studies of (p-Cymene)Ru(Curcuminato)Chloro. *J Med Chem* **2012**, *55*, 1072–1081, doi:10.1021/jm200912j.
50. Pettinari, R.; Marchetti, F.; Di Nicola, C.; Pettinari, C.; Cuccioloni, M.; Bonfili, L.; Eleuteri, A.M.; Therrien, B.; Batchelor, L.K.; Dyson, P.J. Novel Osmium(<scp>ii</Scp>)–Cymene Complexes Containing Curcumin and Bisdemethoxycurcumin Ligands. *Inorg Chem Front* **2019**, *6*, 2448–2457, doi:10.1039/C9QI00843H.
51. Pettinari, R.; Petrini, A.; Marchetti, F.; Di Nicola, C.; Scopelliti, R.; Riedel, T.; Pittet, L.D.; Galindo, A.; Dyson., P.J. Influence of Functionalized η ^{6} -Arene Rings on Ruthenium(II) Curcuminoids Complexes. *ChemistrySelect* **2018**, *3*, 6696–6700, doi:10.1002/slct.201801201.
52. da Silva, B.A.; Pitasse-Santos, P.; Sueth-Santiago, V.; Monteiro, A.R.M.; Marra, R.K.F.; Guedes, G.P.; Ribeiro, R.R.; de Lima, M.E.F.; Decoté-Ricardo, D.; Neves, A.P. Effects of Cu(II) and Zn(II) Coordination on the Trypanocidal Activities of Curcuminoid-Based Ligands. *Inorganica Chim Acta* **2020**, *501*, 119237, doi:10.1016/j.ica.2019.119237.

53. Hussain, A.; Somyajit, K.; Banik, B.; Banerjee, S.; Nagaraju, G.; Chakravarty, A.R. Enhancing the Photocytotoxic Potential of Curcumin on Terpyridyl Lanthanide(<scp>iii</Scp>) Complex Formation. *Dalton Trans.* **2013**, *42*, 182–195, doi:10.1039/C2DT32042H.
54. Banerjee, S.; Prasad, P.; Hussain, A.; Khan, I.; Kondaiah, P.; Chakravarty, A.R. Remarkable Photocytotoxicity of Curcumin in HeLa Cells in Visible Light and Arresting Its Degradation on Oxovanadium(Iv) Complex Formation. *Chemical Communications* **2012**, *48*, 7702, doi:10.1039/c2cc33576j.
55. Halevas, E.; Pekou, A.; Papi, R.; Mavroidi, B.; Hatzidimitriou, A.G.; Zahariou, G.; Litsardakis, G.; Sagnou, M.; Pelecanou, M.; Pantazaki, A.A. Synthesis, Physicochemical Characterization and Biological Properties of Two Novel Cu(II) Complexes Based on Natural Products Curcumin and Quercetin. *J Inorg Biochem* **2020**, *208*, 111083, doi:10.1016/j.jinorgbio.2020.111083.
56. Triantis, C.; Tsotakos, T.; Tsoukalas, C.; Sagnou, M.; Raptopoulou, C.; Terzis, A.; Psycharis, V.; Pelecanou, M.; Pirmettis, I.; Papadopoulos, M. Synthesis and Characterization of *Fac* -[M(CO) $_3$ (P)(OO)] and *Cis-Trans* -[M(CO) $_2$ (P) $_2$ (OO)] Complexes (M = Re, ^{99m} Tc) with Acetylacetone and Curcumin as OO Donor Bidentate Ligands. *Inorg Chem* **2013**, *52*, 12995–13003, doi:10.1021/ic401503b.
57. Rohlíček, J.; Skořepová, E.; Babor, M.; Čejka, J. *CrystalCMP* : An Easy-to-Use Tool for Fast Comparison of Molecular Packing. *J Appl Crystallogr* **2016**, *49*, 2172–2183, doi:10.1107/S1600576716016058.
58. Yan, F.-S.; Sun, J.-L.; Xie, W.-H.; Shen, L.; Ji, H.-F. Neuroprotective Effects and Mechanisms of Curcumin–Cu(II) and –Zn(II) Complexes Systems and Their Pharmacological Implications. *Nutrients* **2017**, *10*, 28, doi:10.3390/nu10010028.
59. Zebib, B.; Mouloungui, Z.; Noirot, V. Stabilization of Curcumin by Complexation with Divalent Cations in Glycerol/Water System. *Bioinorg Chem Appl* **2010**, *2010*, 1–8, doi:10.1155/2010/292760.
60. Khorasani, M.Y.; Langari, H.; Sany, S.B.T.; Rezayi, M.; Sahebkar, A. The Role of Curcumin and Its Derivatives in Sensory Applications. *Materials Science and Engineering: C* **2019**, *103*, 109792, doi:10.1016/j.msec.2019.109792.
61. Shakeri, A.; Panahi, Y.; Johnston, T.P.; Sahebkar, A. Biological Properties of Metal Complexes of Curcumin. *BioFactors* **2019**, *45*, 304–317, doi:10.1002/biof.1504.
62. Shahabadi, N.; Falsafi, M.; Moghadam, N.H. DNA Interaction Studies of a Novel Cu(II) Complex as an Intercalator Containing Curcumin and Bathophenanthroline Ligands. *J Photochem Photobiol B* **2013**, *122*, 45–51, doi:10.1016/j.jphotobiol.2013.03.002.
63. Meza-Morales, W.; Alvarez-Ricardo, Y.; Obregón-Mendoza, M.A.; Arenaza-Corona, A.; Ramírez-Apan, M.T.; Toscano, R.A.; Poveda-Jaramillo, J.C.; Enríquez, R.G. Three New Coordination Geometries of Homoleptic Zn Complexes of Curcuminoids and Their High Antiproliferative Potential. *RSC Adv* **2023**, *13*, 8577–8585, doi:10.1039/d3ra00167a.
64. S., Priya.R.; S., Balachandran.; Daisy, Joseph.; V., Mohanan.P. Reactive Centers of Curcumin and the Possible Role of Metal Complexes of Curcumin as Antioxidants. *Universal Journal of Physics and Application* **2015**, *9*, 6–16, doi:10.13189/ujpa.2015.030102.
65. Jakubczyk, K.; Drużga, A.; Katarzyna, J.; Skonieczna-żydecka, K. Antioxidant Potential of Curcumin—a Meta-Analysis of Randomized Clinical Trials. *Antioxidants* **2020**, *9*, 1–13, doi:10.3390/antiox9111092.
66. Obregón-Mendoza, M.A.; Meza-Morales, W.; Alvarez-Ricardo, Y.; Estévez-Carmona, M.M.; Enríquez, R.G. High Yield Synthesis of Curcumin and Symmetric Curcuminoids: A "Click" and "Unclick" Chemistry Approach. *Molecules* **2022**, *28*, 289, doi:10.3390/molecules28010289.
67. Ng, T.B.; L.F.; W.Z.T. Antioxidative Activity of Natural Products from Plants. *Life Sci* **2000**, *66*, 709–723.
68. Meza-Morales, W.; Alejo-Osorio, Y.; Alvarez-Ricardo, Y.; Obregón-Mendoza, M.A.; Machado-Rodriguez, J.C.; Arenaza-Corona, A.; Toscano, R.A.; Ramírez-Apan, M.T.; Enríquez, R.G. Homoleptic Complexes of Heterocyclic Curcuminoids with Mg(II) and Cu(II): First Conformationally Heteroleptic Case, Crystal Structures, and Biological Properties †. *Molecules* **2023**, *28*, doi:10.3390/molecules28031434.
69. Ohkawa, H.; Ohishi, N.; Yagi, K. Assay for Lipid Peroxides in Animal Tissues by Thiobarbituric Acid Reaction. *Anal Biochem* **1979**, *95*, 351–358, doi:10.1016/0003-2697(79)90738-3.
70. Sheldrick, G.M. *SHELXT* – Integrated Space-Group and Crystal-Structure Determination. *Acta Crystallogr A Found Adv* **2015**, *71*, 3–8, doi:10.1107/S2053273314026370.
71. Sheldrick, G.M. Crystal Structure Refinement with *SHELXL*. *Acta Crystallogr C Struct Chem* **2015**, *71*, 3–8, doi:10.1107/S2053229614024218.
72. Hübschle, C.B.; Sheldrick, G.M.; Dittrich, B. *ShelXle* : A Qt Graphical User Interface for *SHELXL*. *J Appl Crystallogr* **2011**, *44*, 1281–1284, doi:10.1107/S0021889811043202.